DISRUPTION OF SYMPATHETIC OUTFLOW TO INTRA-ABDOMINAL ORGANS EMULATES THE METABOLIC EFFECTS OF SLEEVE GASTRECTOMY IN OBESE MICE

Ana B. Emiliano[1] #, Marko Kraljević[1,2*], Natalie R. Lopatinsky[1], Rogerio B. Oliveira[1], Caroline Jiang[3], Gary J. Schwartz[4] #

1. Columbia University Medical Center, New York, NY, 10032

2. Clarunis, University Center for Gastrointestinal and Liver Diseases, St. Clara Hospital and University Hospital, Basel, Switzerland

3. The Rockefeller University, New York, NY 10061

4. Albert Einstein College of Medicine, New York, NY, 10461

Corresponding author

Corresponding author email address: abe2123@cumc.columbia.edu

Address: 1150 Saint Nicholas Avenue, suite 121, New York, NY 10032

The authors have declared that no conflict of interest exists.

Funding

Berrie Neuroscience of Obesity Initiative at Columbia University - ABE

7K08DK101830-05 – ABE

Berrie Foundation Fellowship Award – MK

Contribution Statement

The first author was responsible for the project conceptualization, design, data acquisition, statistical analysis, and manuscript preparation. The second author was involved in data acquisition and manuscript preparation. The third author was involved in data acquisition. The fifth author participated

in the statistical analysis. The last author provided project conceptualization, design, technical expertise, data interpretation and manuscript editing.

ABSTRACT

Although sleeve gastrectomy (SG) is the most commonly performed bariatric surgery in the US, its mechanistic underpinnings have not been fully determined. Thus, we set out to investigate whether SG's effects on the peripheral sympathetic system could mediate the metabolic effects of SG. The celiac-superior mesenteric ganglia (CSMG) lie juxtaposed to the stomach and supply the sympathetic innervation of the stomach, as well as to numerous other intra-abdominal organs. Here we investigated the effects of SG on the CSMG. SG led to the degeneration of neurons in the CSMG, as evidenced by chromatolysis, which was not found in control mice. Furthermore, CSMG ablation (CGX) completely recapitulated the glycemic and weight loss effects of SG, promoting weight loss at the expense of fat mass. Norepinephrine tissue content measurement by high performance liquid chromatography revealed that liver, duodenum, and ileum were organs where both SG and CGX displayed evidence of significant sympathetic denervation. Both SG and CGX were associated with increased levels of glucagon-like peptide 1 (GLP-1) and high free fatty acid content in the stools. In conclusion, CSMG neuronal degeneration caused by SG may be a partial mediator of the metabolic effects of this type of bariatric surgery.

INTRODUCTION

Despite the popularity of bariatric surgery as a treatment for obesity and type 2 diabetes mellitus (T2DM), the exact mechanisms through which bariatric surgery leads to glycemic improvement and durable weight loss are largely unknown. The potential involvement of the vagal motor and sensory innervation of the stomach and other parts of the gastrointestinal (GI) tract in the achievement of the beneficial metabolic outcomes of bariatric surgery has garnered substantial attention in the preclinical literature, especially in relation to RYGB (1-5). The rationale for this emphasis on studying the effects of bariatric surgery on the vagal innervation stem in part from the rich vagal sensory motor innervation

of the stomach (6) and the fact that vagal sensory terminals have the important function of detecting changes in pressure, volume and nutrient exposure (7). However, the stomach also receives rich sympathetic innervation, mainly from the celiac-superior mesenteric ganglia (CSMG) (8). The CSMG are prevertebral sympathetic ganglia classically believed to transduce central nervous system (CNS) input to the target organs it innervates, which include liver, pancreas, stomach, intestines, kidneys, and adrenal glands (9-12). Much less is known about the potential role played by sympathetic CSMG neurons in obesity or metabolic disease. Sympathetic nervous system (SNS) overactivity is a hallmark of obesity accompanied by the metabolic syndrome (13). Weight loss, either through lifestyle modifications or sleeve gastrectomy (SG), has been shown to reduce SNS activity, while also decreasing cardiovascular mortality and improving glucose homeostasis (14, 15). Increased SNS activity has been linked to insulin resistance (16, 17) and to negative clinical outcomes in heart failure, kidney disease, coronary artery disease and stroke (18-21). A recent study pointed to the potential involvement of CSMG neurons in glucose homeostasis via input received from cocaine- and amphetamine- regulated transcript^{+}(CART) viscerofugal neurons in the intestine (22). CSMG neurons have also been implicated in the sympathoadrenal response to hypoglycemia, as CSMG ganglionectomy (CGX) in rats led to a 50% decrease in the epinephrine and norepinephrine response to insulin-induced hypoglycemia (23). It is not known, however, whether sympathetic ganglia are mediators of the deleterious effects imparted by sympathetic overactivity on cardiovascular and metabolic function in obesity. Furthermore, although a decrease in leptin and insulin plasma levels that results from weight loss are thought to be linked to the SNS decline in activity after any type of weight loss, the exact mechanisms through which weight loss promotes SNS inhibition remain largely undetermined. Moreover, it is not known if SG decreases SNS activity through direct, weight loss independent mechanisms.

Consequently, using 18-week-old wild type, diet-induced obese (DIO) mice, we set out to investigate whether SG exerted any effects on the CSMG and whether these effects were could be related to SG-induced blood glucose lowering and weight loss.

Material and Methods

Animals, Housing and Experimental Design

The studies were performed according to ARRIVE guidelines and in accordance with the Columbia University Institutional Animal Care and Use Committee, which granted approval for all the experiments in this study. Female C57bl/6J mice were purchased from The Jackson Laboratories at 6 weeks of age and maintained thereafter on a high fat diet (Research Diets, catalogue number D12492, New Jersey, NJ). C57bl/6J obese female mice are not commercially available. Male C57bl/6J raised on a 60% high fat diet from 6 weeks of age, were purchased from The Jackson Laboratories at 15-16 weeks of age and maintained on a high fat diet throughout all studies. Mice were group housed in a vivarium maintained at 22°C on a 12:12 (7 am - 7 pm) light / (7 pm - 7 am) dark cycle. At 18 weeks of age, mice were randomized to SG (sleeve gastrectomy group), CGX (CSMG ablation group), SH-IF weight matched to the SG group (sham surgery with caloric restriction and intermittent fasting) and SH-AL (sham surgery with ad libitum feeding) (n=8-14 for SG; n=8-12 for SH-IF, n=8-12 for SH-AL, for both male and female cohorts). Intermittent fasting (IF) involved feeding the SH-IF group a variable ration, once daily, at different times of the day, on weekdays, with the amount depending on their weight loss or gain, so that they would be weight-matched to the SG group. From Fridays to Mondays, SH-IF mice were allowed to eat without restriction (*ad libitum*). Baseline measurements were defined as having been taken approximately 2 weeks prior to surgeries. Body weight (BW) and food intake were measured daily for the first week post-operatively and weekly thereafter. For experiments that involved perfusion, mice at 4 weeks post-surgery were placed under isoflurane anesthesia, after an overnight fast (8-10 hours), and intracardiac perfusion was performed with 0.9% saline, followed by 4% paraformaldehyde, and the liver was harvested for tissue clearing (iDisco, see below). For CSMG microscopy, the CSMG from mice that underwent SG, SH-AL and SH-IF were dissected from mice who were under isoflurane anesthesia, placed in 4% paraformaldehyde overnight and transferred to 30% sucrose for 2 days before being frozen for section in a cryostat. The mice were subsequently euthanized by cervical dislocation.

Surgical Procedures. Sleeve gastrectomy was performed in anesthetized mice (isoflurane) to remove approximately 80% of the stomach, as previously described previously (24, 25). For the sham surgery, a laparotomy was followed by isolation of the stomach, severance of the gastrosplenic and gastrophrenic ligaments, followed by exertion of pressure with a smooth forceps along a vertical line between the esophageal sphincter and the pylorus, at the point where the stomach is resected in the VSG procedure. The stomach was placed back into the abdominal cavity and the laparotomy closed in layers. CGX was performed by carefully dissecting all the nerve tissue lying between and around the celiac artery and superior mesenteric artery, and which also encroaches on the abdominal aorta (figure 1).

Glucose Tolerance Test and Insulin Tolerance Test

Mice were fasted for 6 hours prior to glucose and insulin tolerance tests. SH-IF mice were fed from 0.8-1.0 g of high fat diet one hour prior to the start of the 6-hour fast, in preparation for the glucose and insulin tolerance tests. This was done to avoid a more prolonged period of fasting in SH-IF mice, compared to SG and SH-AL mice. Oral glucose tolerance tests were performed at baseline, and then at 1, 4, and 8 weeks post-operatively; insulin tolerance tests were performed 4 weeks post-operatively. Oral glucose tolerance tests (OGTT) were performed by oral gavage using a plastic feeding tube (1FTP-20-38, Instech Laboratories, Inc.), with 2 grams of dextrose per kg of body weight. Insulin tolerance tests (ITT) were performed using regular insulin at a dose of 0.75 units per Kg of body weight, injected intraperitoneally (Humulin R, Lilly).

Body Composition, Energy expenditure and Locomotor Activity

Body composition was measured weekly post-operatively using Echo-MRI™-100H (EchoMRI LLC, Houston, TX). Energy expenditure by indirect calorimetry was performed by singly housing mice in the Comprehensive Lab Animal Monitoring System (CLAMS, Columbus Instruments, Columbus, OH) for one week, between 3-4 weeks post-operatively. The SH-IF group was fed ad libitum during the calorimetry experiment. CLAMS measurements included Volume O_2, O_2 in and O_2 out, delta O_2, Accumulated O_2, Volume CO_2, CO_2 in and CO_2 out, delta CO_2, Accumulated CO_2, RER, Heat, Flow,

Feed Weight, Feed Accumulation, and Total Locomotor Activity, which was calculated as the sum of activity along the X, Y and Z axes of the chambers.

Fecal Free-Fatty Acid Content Assay

Feces were collected from individual mice at 1, 2 and 4 weeks post-operatively (they were not collected during the third week because the mice were in the indirect calorimetry cages). Feces were dried overnight on a six-well plate, at 42ºC. For each reaction, 100 mg of feces (per mouse) were placed in 1 mL of NaCl and then homogenized with beads for five minutes. The solution was transferred to a 15 mL tube, to which a mix of chloroform and methanol at 2:1 was added (Chloroform, Fisher, C298-4; Methanol, Fisher A456-212). The mixture was vortexed vigorously and then centrifuged at 2000g for 10 minutes. The chloroform phase was collected and transferred to a 20 mL vial and evaporated under dinitrogen. After that, 1 mL of deionized water was added. The next day, samples were assayed in duplicates, with a Free Fatty Acid (FFA) kit (Wako 995-34693; 997-34893; Fujifilm USA). Samples were diluted at 1:20 and incubated at 37ºC for five minutes and read with a microplate reader.

Tissue Norepinephrine Content

Liver, pancreas, duodenum, jejunum, ileum, mesenteric white adipose tissue (mWAT), inguinal white adipose tissue (iWAT), gonadal white adipose tissue (gWAT) and interscapular brown adipose tissue (iBAT) were collected 4 weeks post-surgery from overnight fasted mice (8-10 hours) and immediately frozen on dry ice and transferred to a minus 80 freezer. Tissues were then homogenized for measurement of norepinephrine by high performance liquid chromatography, as previously described (26).

Plasma Assays

At 2 weeks post-surgery, blood was collected via intracardiac puncture from overnight fasted mice (8-10 hours). A separate group of mice were also fasted overnight (8-10 hours) and euthanized 30 minutes after receiving an oral gavage with 200 µL of Ensure, and their blood was collected via cardiac puncture. Blood was placed in serum separator tubes (Microvette, Kent Scientific catalogue #MTSC-SER), to which aprotinin, diprotin A (a DPPIV inhibitor) and Halt protease inhibitor cocktail were added (aprotinin,

Millipore Sigma, catalogue #A1153; diprotin A, Enzo Scientific, catalogue #ALX-260-036-M005; HALT, Thermo Scientific catalogue # PI87785). Blood was spun for 15 min at 2000 g in a refrigerated benchtop microcentrifuge and subsequently stored at -80°C. Serum Leptin, insulin, active GLP-1, and Ghrelin were measured using a U-PLEX MSD assay (MesoScale Discovery, catalogue # K152ACM-1).

Cholera toxin B injections in liver, pancreas, and mesenteric white adipose tissue

Cholera toxin B (CTb) conjugated with Alexa fluor 647 and 555 were injected into the liver parenchyma (total of 15 µL split through liver segments) and pancreas (total of 10 µL divided into head, body, and tail), respectively (Invitrogen, 647, #C34778; Invitrogen, 555, # C34776). Then, in a separate experiment, CTb conjugated with Alexa Fluor 647 was injected into the mesenteric white adipose tissue (mWAT) (10 µL total). In a third experiment, mice were injected with CTb conjugated with Alexa Fluor 488, 555 and 647 in pancreas, liver and mWAT, respectively, in the same manner as described above (CTb Invitrogen, 488, # C34775). Mice were euthanized 5 days after CTb injections, their CSMG harvested, fixed overnight in fresh 4% paraformaldehyde, and transferred to 30% sucrose. Whole CSMG were processed for iDisco as previously described (27).

Imaging Experiments

Liver iDisco was performed as previously described (28). Primary antibodies were anti-Protein Gene Product 9.5 (PGP9.5) (Invitrogen, #PA1-10011) and anti-Tyrosine Hydroxylase (TH) (Millipore, #AB152) at 1:200 dilution for both antibodies. Secondary antibodies were Alexa Fluor 647 Goat anti-Chicken (Invitrogen, #A-21449) and Alexa Fluor 790 Goat anti-Rabbit (Invitrogen, #A11369) at 1:200 dilution for both antibodies. Images were obtained using a Ultramicroscope II Light sheet microscope (2x0.5NA objective, with a 1X zoom) and analyzed using Imaris software according (Imaris 9.2 Reference Manual). iDisco images presented in this manuscript are raw data.

For the detection of neuronal degeneration, CSMG were cut in 20 µm sections with a cryostat. Sections were then stained with the fluorescence Nissl stain NeuroTrace 640/660 Deep Red fluorescence (Invitrogen, catalogue #N21483) at a dilution of 1:300 and counterstained with DAPI (ThermoScientific,

#62247). Prolong Diamond antifade mountant (Invitrogen, # P36970) was used for cover slipping. Images were taken with a spinning disk confocal microscope, at 20X magnification.

Statistics

We used GraphPad Prism 9 version software. Data from female and male mice experiments were analyzed separately. Non-parametric Mann Whitney tests were used for two-group comparisons of a single measure. One-way ANOVA with Kruskal-Wallis tests were used for comparisons of single measures among more than two groups. Two-way ANOVA with Multiple Comparisons with Tukey tests were used for analysis of multiple groups involving repeated measures. Data are expressed as means ± SEM. Area Under the Curve (AUC) was generated for OGTT and ITT and then compared using Two-way ANOVA with Multiple Comparisons and Tukey tests. Column factor refers to surgical group and row factor to time. Generalized Linear Model in SPSS was used for TEE analysis, which included adjustment for fat-free mass and fat mass. For all analyses, power was set at 80%, with a p value of <0.05.

The analysis of liver sympathetic innervation after tissue clearing was performed using the Imaris software function 'filament length' and 'filament volume'. A mixed model and mixed effects model was used to analyze the liver innervation data.

Results

SG leads to CSMG neuronal degeneration

Four weeks post-surgery, neuronal degeneration can be observed in the CSMG of SG mice, as evidenced by the presence of chromatolysis (figure 2A). No evidence of chromatolysis was found in SH-AL or SH-IF mice (figure 2B). During chromatolysis, there is dissolution/loss of the Nissl substance (rough endoplasmic reticulum or RER), nuclear eccentricity, nuclear, nucleolar, and cytoplasmic swelling (figure 2C) (29). Target organs innervated by the degenerated nerve cell may lose their innervation unless the neurons regenerate (figure 2D).

CGX recapitulates the weight loss effects of SG

Percent weight change was similar for male SG and CGX mice, and significantly lower than both the SH-AL and SH-IF groups initially (Fig.3A) (For a and b, $p<0.0001$ on week 1, 2, 3 and 4. For a and c, $p<0.05$). By the 4th week post-surgery, SH-IF caught up with the percent weight loss of SG and CGX mice, while SH-AL did not. Percent Fat Mass (FM) change followed the same pattern, showing that weight loss in SG and CGX mice occurred at the expense of FM (figure 3B) (For a and b, $p <0.05$ for week 1; $p<0.001$ for week 2; $p<0.0001$ for week 3, $p<0.05$ for week 4. For a and c, $p<0.001$). For Lean Mass (LM) change, the inverse pattern occurred for SG and CGX versus SH-IF, with the first two conditions increasing LM over time, while LM losses became more severe for SH-IF (figure 3C) (For a and b, $p<0.0001$ for week 2 and 3; and $p<0.001$ for week 4). SH-AL never lost any LM, and instead gained significant LM. Two-way ANOVA with multiple comparisons was used for these analyses. Weight loss was equally significant in female CGX mice (supplemental figure 1A). Serum leptin (figure 3D) was significantly higher in SH-AL, which correlated well with their body weight and fat mass. Serum leptin in SH-IF was also elevated on the account of two outliers.

SG, CGX and SH-IF lead to similar improvements in glucose homeostasis

Baseline OGTT, expressed as area under the curve (AUC), was similar for female and male cohorts (supplemental figure 2, Two-way ANOVA with multiple comparisons with Tukey test, for baseline $p>0.05$). OGTT AUC improved remarkably in the first week post-surgery for male SG, CGX and SH-IF mice compared to SH-AL's glucose tolerance (figure 4A and C, One-way ANOVA was used for analysis of AUC. For A, $p<0.001$; for B, $p<0.0001$; for C, $p<0.05$; for D, $p<0.01$). Insulin sensitivity (Fig 4B and D) was slightly better for male CGX mice, compared to SG mice, and similar to SH-IF mice (One-way ANOVA was used for analysis of AUC. For A, $p<0.001$; for B, $p<0.0001$; for C, $p<0.05$; for D, $p<0.01$). In week 4, male CGX, SG and SH-IF mice had equivalent insulin sensitivity. Throughout the study, male SH-AL mice had worse glucose tolerance and insulin sensitivity than all the other groups. While

CGX, SG and SH-IF had robust effects in terms of glucose homeostasis improvement in male mice, we did not observe significant effects in females (supplemental figure 1B, C and D).

During a mixed meal test, CGX mice were found to have a significantly elevated fasting serum active GLP-1 levels compared to SG and controls, whereas the 30-minute stimulated time point (after an oral gavage with 200 µl of Ensure) was not significantly higher than the baseline (fasting point), but higher than in control mice (figure 4E) (One-way ANOVA, $p<0.05$ for CGX versus SG, and $p<0.01$ for CGX versus SH-AL and SH-IF). Serum insulin was significantly higher in SH-AL mice in the fasting state, and only slightly elevated in CGX and SG mice at 30 minutes compared to the baseline value but not significantly so (figure 4F) (One-way ANOVA, SH-AL versus other groups $p<0.05$).

Fecal free fatty acid loss occurs in CGX and SG mice

The significant weight loss experienced by male CGX and SG mice does not appeared to be linked to any significant reduction in energy intake (figure 5A) (For a and b, $p<0.01$ for week 1, $p<0.0001$ for week 2, and $p<0.05$ for week 3. For a and c, $p<0.01$ for week 1, $p<0.05$ for week 2 and 3. For a and d, $p<0.001$ for week 2 and $p<0.0001$ for week 4. Two-way ANOVA with multiple comparisons, column factor $F (3, 104) = 31.98$). Fat-free Mass adjusted total energy expenditure was similar across the 4 groups, also not explaining the lower body weight in CGX and SG mice (figure 5B, nonsignificant, linear regression model, SPSS). Fecal free fatty acid content was similar across the groups on week 1 (figure 5C), but higher in SG and CGX in weeks 2 and 4 (figure 5D and E) (One-way ANOVA. N=7-9; * for $p<0.05$, ** $p<0.01$, *** $p<0.001$ and $p<0.0001$). Serum ghrelin at fasting and 30 min after an oral gavage with 200 µL of Ensure did not reveal any significant differences among the groups, suggesting that ghrelin is not an important mediator of appetite regulation in these mice (figure 5F) (One-way ANOVA, $p>0.05$).

Sympathetic denervation in the liver of CGX and SG mice

As we hypothesized that sympathetic neuronal degeneration in the CSMG partially mediates the weight loss and glycemic effects of SG, we measured tissue norepinephrine content as a surrogate for sympathetic denervation (figure 6A)(Two-way ANOVA with multiple comparisons; N=5 mice per group; for liver, a and b, $p<0.05$; for pancreas, a and b, $p<0.01$; for duodenum, a and b, $p<0.05$, and a and c, $p<0.001$; for jejunum, $p>0.05$; for ileum, a and b, $p<0.01$, and for a and c, $p<0.001$; for mWAT, a and b, $p<0.01$, and a and c, $p<0.05$; for iWAT, gWAT and iBAT, $p>0.05$). We measured norepinephrine content in liver, pancreas, duodenum, jejunum, ileum, mWAT, iWAT, gWAT and iBAT. We included mWAT because our CTb tracing studies revealed that CSMG neurons innervate that adipose tissue depot (supplemental figure 3). Although the CSMG do not innervate iWAT, gWAT, or iBAT, we included those tissues in the analysis, as their sympathetic innervation could have been affected through indirect pathways. The data from the tissue norepinephrine content suggested that in male mice, sympathetic denervation of the liver, duodenum, and ileum were common features shared by CGX and SG mice. SG's liver norepinephrine content was in-between the level for CGX and the level for control mice. SH-IF mice, who towards the end of the period of study observation had lost significant amounts of weight, overall, also displayed decreased tissue norepinephrine content compared to SH-AL mice, who did not lose any significant amount of weight. Regarding mWAT, the CGX group had the lowest tissue norepinephrine content. No significant findings were associated with iWAT, gWAT or iBAT in any groups.

Because of the importance of the liver in maintaining systemic glucose homeostasis, we further sought to determine whether SG decreases in hepatic sympathetic innervation density. Using iDisco tissue clearing we found that SG mice had lower filament length and filament volume, compared SH-AL and SH-IF mice (figure 6B and C) (Mixed model and mixed effects model analysis, $p<0.05$ for both length and volume, normalized by area). In figure 6B, SG images show a low density of axons, compared to SH-AL and SH-IF mice, observed in PGP9.5 labeling, TH-labeling, and the merging of both.

Discussion

This is the first study to demonstrate the effects of SG on the CSMG, the major prevertebral sympathetic ganglia innervating the gastric target of this bariatric procedure. Chromatolysis in the CSMG of SG mice was not simply the result of laparotomy or abdominal manipulation, as mice that underwent sham surgery had no evidence of neuronal degeneration in their CSMG. We are not the first group to demonstrate that resection of stomach tissue can lead to neuronal degeneration of the sympathetic ganglia supplying its innervation. Gerke (30) demonstrated that in dogs that undergo total gastrectomy, chromatolysis and apoptosis of CSMG neurons can be shown up to one year following the surgery. Our study does not demonstrate apoptosis and we did not perform comparative neuronal cell counts to be able to state that SG leads to neuronal cell death. Ongoing studies will be able to make that determination in the near future. The question is whether this finding has biological and clinical relevance. Based on the finding that CSMG ablation (CGX) in obese mice recapitulates the glycemic and weight loss effects of SG suggests that neuronal degeneration is important for SG's metabolic effects. A recent study that investigated the role of cannabinoid signaling in the weight loss and glycemic effects of RYGB found that splanchnic denervation causes weight loss and blood glucose improvement in obese mice (31). It is not known how splanchnic denervation and CGX differ, since the splanchnic nerve carries CNS input to CSMG neurons. It is likely that CGX is more effective in causing widespread sympathetic denervation in the abdominal organs it innervates (32). Importantly, the present results support the idea that inhibition of sympathetic drive in obesity appears to alleviate hyperglycemia and promote weight loss.

CGX has been shown to decrease arterial pressure in rodent models of hypertension, underscoring the role CSMG neurons play in regulating cardiovascular function, as they supply innervation to the splanchnic circulation (33, 34). This finding further suggests involvement of CSMG neurons in states of SNS overactivity, such as hypertension. We now demonstrate that ablation of CSMG neurons also ameliorates another state of SNS overactivity, which is obesity with hyperglycemia. CGX in obese mice led to weight loss and fat mass loss that was equivalent to those

achieved through SG. This loss did not appear to be secondary to any significant effects of CGX on energy intake or energy expenditure. However, it is important to point out that CGX did not lead to metabolic adaptation, as defined by a loss of FFM accompanied by a reduction in energy expenditure and weight regain. Metabolic adaptation is a hallmark of diet-induced weight loss in humans and rodents(35, 36), and is partly attributable to a decline in skeletal muscle energy expenditure, occurring even after modest weight loss, defined as less than a 10% loss of body weight (37, 38).

Results from the present study suggest that weight loss in CGX and SG is importantly related to increased fecal calorie excretion, as evidenced by the high free fatty acid content in the stools of CGX and SG mice. This points to a malabsorptive phenotype in both CGX and SG mice, consistent with the changes in sympathetic innervation in the duodenum and ileum that we found in the present study. Future studies need to address whether the fat malabsorption phenotype we found is secondary to bile acid malabsorption, impaired nutrient absorption, or microbiome changes. Although SG is not classically viewed as a malabsorptive procedure, recent studies have revealed that SG in humans is associated with evidence of malabsorption of oral anticoagulants and birth control pills (39, 40).

CGX in obese mice was also associated with improved glucose homeostasis. It is not clear whether CGX's effects on blood glucose are weight-loss independent. CGX led to increased serum levels of active GLP-1, although, unlike SG, the levels were already elevated at baseline, when the mice were fasting. Future studies will need to evaluate whether increased GLP-1 secretion is a mechanism through which CGX influences glucose homeostasis, independently of CGX-induced weight loss. Other potential mechanisms for CGX to ameliorate blood glucose independent of weight loss include liver, pancreas and mWAT sympathetic denervation, which the low norepinephrine content in those tissues suggest are important contributing factors. Neurons in the CSMG are the main source of adrenergic efferent projections to the liver (9, 10). Autonomic input descending from the hypothalamus and transmitted through efferent projections in the periphery regulates liver glycogen metabolism(41). Increased sympathetic outflow to liver results in an increase in hepatic glucose output(42). This occurs due to the stimulation of hepatic glycogen phosphorylase and

phosphoenolpyruvate carboxykinase, which promote glycogenolysis and gluconeogenesis, respectively(43). The pancreas also receives adrenergic innervation that originates in the CSMG(8). When the CSMG is resected in rats, only 10% of adrenergic axons are left in the pancreas, confirming that the CSMG is the main source of pancreatic sympathetic innervation(11). The pancreatic islets are abundantly innervated, as first recognized by Langerhans(44). While the pancreatic parasympathetic innervation in humans, compared to mice, is sparser, adrenergic fibers richly innervate arterioles, capillaries, and the islets in both humans and rodents(45). Stimulation of α adrenergic receptors on pancreatic beta cells leads to potent inhibition of insulin secretion(46, 47). On the other hand, beta adrenergic receptor stimulation on pancreatic alpha cells promotes glucagon secretion(48). Despite significant advances in the understanding of hepatic and pancreatic sympathetic innervation, little is known about whether there is a direct role for CSMG neurons in metabolic regulation or whether specific CSMG neuronal populations are specialized in the regulation of hepatic or pancreatic function. Regarding mWAT function, it is the only visceral adipose tissue depot that is equivalent in humans and rodents(49). Using Pseudorabies virus tracing, Nguyen *et al* found that mWAT is innervated by the sympathetic chain ganglia (T5-L3)(50). However, in that study, the CSMG was not checked for labeling. In the present manuscript, we report that we found that CSMG neurons innervate mWAT. Moreover, we found that CSMG neurons projecting to liver, pancreas and mWAT are mostly specific, rarely co-localizing.

Finally, while the weight loss effects of CGX in females are similar to what is observed in males, CGX did not promote significant improvement in glucose homeostasis in females. Future work is needed to identify and characterize the neurobiological and neuroendocrine bases for this apparent sex-based difference.

In summary, our study reveals a new potential mechanism, CSMG neuronal degeneration, that mediates the metabolic benefits of SG, specifically in the obese state.

References

1. Shin AC, Zheng H, and Berthoud HR. Vagal innervation of the hepatic portal vein and liver is not necessary for Roux-en-Y gastric bypass surgery-induced hypophagia, weight loss, and hypermetabolism. *Ann Surg.* 2012;255(2):294-301.
2. Hao Z, Townsend RL, Mumphrey MB, Patterson LM, Ye J, and Berthoud HR. Vagal innervation of intestine contributes to weight loss After Roux-en-Y gastric bypass surgery in rats. *Obes Surg.* 2014;24(12):2145-51.
3. Gautron L, Zechner JF, and Aguirre V. Vagal innervation patterns following Roux-en-Y gastric bypass in the mouse. *Int J Obes (Lond).* 2013;37(12):1603-7.
4. Wierdak M, Korbut E, Hubalewska-Mazgaj M, Surmiak M, Magierowska K, Wojcik-Grzybek D, et al. Impact of Vagotomy on Postoperative Weight Loss, Alimentary Intake, and Enterohormone Secretion After Bariatric Surgery in Experimental Translational Models. *Obes Surg.* 2022;32(5):1586-600.
5. Ballsmider LA, Vaughn AC, David M, Hajnal A, Di Lorenzo PM, and Czaja K. Sleeve gastrectomy and Roux-en-Y gastric bypass alter the gut-brain communication. *Neural Plast.* 2015;2015:601985.
6. Powley TL, Jaffey DM, McAdams J, Baronowsky EA, Black D, Chesney L, et al. Vagal innervation of the stomach reassessed: brain-gut connectome uses smart terminals. *Ann N Y Acad Sci.* 2019;1454(1):14-30.
7. Williams EK, Chang RB, Strochlic DE, Umans BD, Lowell BB, and Liberles SD. Sensory Neurons that Detect Stretch and Nutrients in the Digestive System. *Cell.* 2016;166(1):209-21.
8. Quinson N, Robbins HL, Clark MJ, and Furness JB. Locations and innervation of cell bodies of sympathetic neurons projecting to the gastrointestinal tract in the rat. *Arch Histol Cytol.* 2001;64(3):281-94.
9. Uyama N, Geerts A, and Reynaert H. Neural connections between the hypothalamus and the liver. *Anat Rec A Discov Mol Cell Evol Biol.* 2004;280(1):808-20.
10. Torres H, Huesing C, Burk DH, Molinas AJR, Neuhuber WL, Berthoud HR, et al. Sympathetic innervation of the mouse kidney and liver arising from prevertebral ganglia. *Am J Physiol Regul Integr Comp Physiol.* 2021;321(3):R328-R37.
11. Anglade P, Michel C, and Roze C. Intrinsic nerves of the pancreas after celiac and superior mesenteric ganglionectomy in rats: a morphologic study of acetylcholinesterase activity and catecholamine histofluorescence. *Pancreas.* 1987;2(5):568-77.
12. Hayakawa T, Kuwahara S, Maeda S, Tanaka K, and Seki M. Morphology and ultrastructure of the sympathetic celiac ganglion neurons projecting to the cardia and pylorus of the rat stomach. *Auton Neurosci.* 2007;134(1-2):8-17.
13. Lambert GW, Straznicky NE, Lambert EA, Dixon JB, and Schlaich MP. Sympathetic nervous activation in obesity and the metabolic syndrome--causes, consequences and therapeutic implications. *Pharmacol Ther.* 2010;126(2):159-72.
14. Mark AL. Weight reduction for treatment of obesity-associated hypertension: nuances and challenges. *Curr Hypertens Rep.* 2007;9(5):368-72.
15. Seravalle G, Colombo M, Perego P, Giardini V, Volpe M, Dell'Oro R, et al. Long-term sympathoinhibitory effects of surgically induced weight loss in severe obese patients. *Hypertension.* 2014;64(2):431-7.
16. Lembo G, Capaldo B, Rendina V, Iaccarino G, Napoli R, Guida R, et al. Acute noradrenergic activation induces insulin resistance in human skeletal muscle. *Am J Physiol.* 1994;266(2 Pt 1):E242-7.

17. Jamerson KA, Julius S, Gudbrandsson T, Andersson O, and Brant DO. Reflex sympathetic activation induces acute insulin resistance in the human forearm. *Hypertension.* 1993;21(5):618-23.
18. Cohn JN, Levine TB, Olivari MT, Garberg V, Lura D, Francis GS, et al. Plasma norepinephrine as a guide to prognosis in patients with chronic congestive heart failure. *N Engl J Med.* 1984;311(13):819-23.
19. Zoccali C, Mallamaci F, Parlongo S, Cutrupi S, Benedetto FA, Tripepi G, et al. Plasma norepinephrine predicts survival and incident cardiovascular events in patients with end-stage renal disease. *Circulation.* 2002;105(11):1354-9.
20. Rouleau JL, Packer M, Moye L, de Champlain J, Bichet D, Klein M, et al. Prognostic value of neurohumoral activation in patients with an acute myocardial infarction: effect of captopril. *J Am Coll Cardiol.* 1994;24(3):583-91.
21. Sander D, Winbeck K, Klingelhofer J, Etgen T, and Conrad B. Prognostic relevance of pathological sympathetic activation after acute thromboembolic stroke. *Neurology.* 2001;57(5):833-8.
22. Muller PA, Matheis F, Schneeberger M, Kerner Z, Jove V, and Mucida D. Microbiota-modulated CART(+) enteric neurons autonomously regulate blood glucose. *Science.* 2020;370(6514):314-21.
23. Fujita S, and Donovan CM. Celiac-superior mesenteric ganglionectomy, but not vagotomy, suppresses the sympathoadrenal response to insulin-induced hypoglycemia. *Diabetes.* 2005;54(11):3258-64.
24. Garibay D, and Cummings BP. A Murine Model of Vertical Sleeve Gastrectomy. *J Vis Exp.* 2017(130).
25. Emiliano AB, Lopatinsky NR, Kraljevic M, Higuchi S, He Y, Haeusler RA, et al. Sex-specific differences in metabolic outcomes after sleeve gastrectomy and intermittent fasting in obese middle-aged mice. *Am J Physiol Endocrinol Metab.* 2022;323(1):E107-E21.
26. De Benedetto GE, Fico D, Pennetta A, Malitesta C, Nicolardi G, Lofrumento DD, et al. A rapid and simple method for the determination of 3,4-dihydroxyphenylacetic acid, norepinephrine, dopamine, and serotonin in mouse brain homogenate by HPLC with fluorimetric detection. *J Pharm Biomed Anal.* 2014;98:266-70.
27. Renier N, Wu Z, Simon DJ, Yang J, Ariel P, and Tessier-Lavigne M. iDISCO: a simple, rapid method to immunolabel large tissue samples for volume imaging. *Cell.* 2014;159(4):896-910.
28. Liu K, Yang L, Wang G, Liu J, Zhao X, Wang Y, et al. Metabolic stress drives sympathetic neuropathy within the liver. *Cell Metab.* 2021;33(3):666-75 e4.
29. McIlwain DL, and Hoke VB. The role of the cytoskeleton in cell body enlargement, increased nuclear eccentricity and chromatolysis in axotomized spinal motor neurons. *BMC Neurosci.* 2005;6:19.
30. Gerke RP. [Morphological changes in nodes of the celiac plexus as affected by extensive abdominal surgery]. *Biull Eksp Biol Med.* 1984;97(3):370-3.
31. Ye Y, Abu El Haija M, Morgan DA, Guo D, Song Y, Frank A, et al. Endocannabinoid Receptor-1 and Sympathetic Nervous System Mediate the Beneficial Metabolic Effects of Gastric Bypass. *Cell Rep.* 2020;33(4):108270.
32. Li M, Galligan J, Wang D, and Fink G. The effects of celiac ganglionectomy on sympathetic innervation to the splanchnic organs in the rat. *Autonomic neuroscience : basic & clinical.* 2010;154:66-73.
33. Asirvatham-Jeyaraj N, Gauthier MM, Banek CT, Ramesh A, Garver H, Fink GD, et al. Renal Denervation and Celiac Ganglionectomy Decrease Mean Arterial Pressure Similarly in Genetically Hypertensive Schlager (BPH/2J) Mice. *Hypertension.* 2021;77(2):519-28.
34. King AJ, Osborn JW, and Fink GD. Splanchnic circulation is a critical neural target in angiotensin II salt hypertension in rats. *Hypertension.* 2007;50(3):547-56.
35. Leibel RL, and Hirsch J. Diminished energy requirements in reduced-obese patients. *Metabolism.* 1984;33(2):164-70.
36. Johannsen DL, Knuth ND, Huizenga R, Rood JC, Ravussin E, and Hall KD. Metabolic slowing with massive weight loss despite preservation of fat-free mass. *J Clin Endocrinol Metab.* 2012;97(7):2489-96.

37. Doucet E. Greater than predicted decrease in energy expenditure during exercise after body weight loss in obese men. *Clinical Science.* 2003;105:89-95.
38. Weiss EP, Jordan RC, Frese EM, Albert SG, and Villareal DT. Effects of Weight Loss on Lean Mass, Strength, Bone, and Aerobic Capacity. *Med Sci Sports Exerc.* 2017;49(1):206-17.
39. Rottenstreich A, Barkai A, Arad A, Raccah BH, and Kalish Y. The effect of bariatric surgery on direct-acting oral anticoagulant drug levels. *Thromb Res.* 2018;163:190-5.
40. Goldenshluger A, Elazary R, Ben Porat T, Farhat HG, Levin G, and Rottenstreich A. Knowledge, attitudes, and behaviors of women during pregnancy after bariatric surgery. *Surg Obes Relat Dis.* 2020;16(7):925-30.
41. Shimazu T, Fukuda A, and Ban T. Reciprocal influences of the ventromedial and lateral hypothalamic nuclei on blood glucose level and liver glycogen content. *Nature.* 1966;210(5041):1178-9.
42. Shimazu T, and Fukuda A. Increased activities of glycogenolytic enzymes in liver after splanchnic-nerve stimulation. *Science.* 1965;150(3703):1607-8.
43. Shimazu T. Neuronal regulation of hepatic glucose metabolism in mammals. *Diabetes Metab Rev.* 1987;3(1):185-206.
44. P L. Contributions to the microscopic anatomy of the pancreas. *Baltimore: The Johns Hopkins Press.* 1937.
45. Chien HJ, Chiang TC, Peng SJ, Chung MH, Chou YH, Lee CY, et al. Human pancreatic afferent and efferent nerves: mapping and 3-D illustration of exocrine, endocrine, and adipose innervation. *Am J Physiol Gastrointest Liver Physiol.* 2019;317(5):G694-G706.
46. Porte D, Jr. Sympathetic regulation of insulin secretion. Its relation to diabetes mellitus. *Arch Intern Med.* 1969;123(3):252-60.
47. Imura H, Kato Y, Ikeda M, Morimoto M, and Yawata M. Effect of adrenergic-blocking or -stimulating agents on plasma growth hormone, immunoreactive insulin, and blood free fatty acid levels in man. *J Clin Invest.* 1971;50(5):1069-79.
48. Schuit FC, and Pipeleers DG. Differences in adrenergic recognition by pancreatic A and B cells. *Science.* 1986;232(4752):875-7.
49. Catalano KJ, Stefanovski D, and Bergman RN. Critical role of the mesenteric depot versus other intra-abdominal adipose depots in the development of insulin resistance in young rats. *Diabetes.* 2010;59(6):1416-23.
50. Nguyen NL, Randall J, Banfield BW, and Bartness TJ. Central sympathetic innervations to visceral and subcutaneous white adipose tissue. *Am J Physiol Regul Integr Comp Physiol.* 2014;306(6):R375-86.

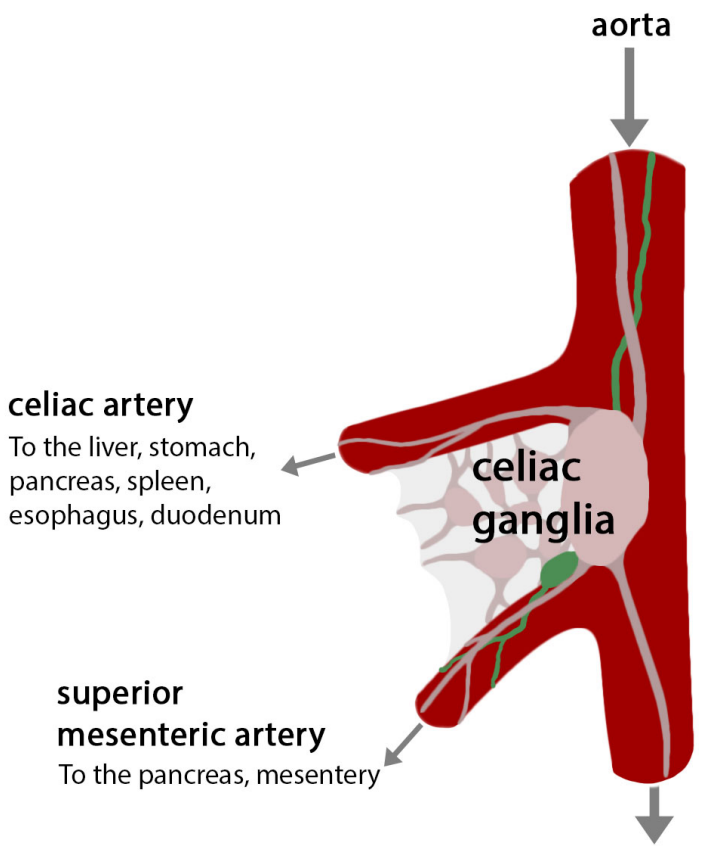
aorta
celiac artery
To the liver, stomach, pancreas, spleen, esophagus, duodenum
celiac ganglia
superior mesenteric artery
To the pancreas, mesentery

Figure 1

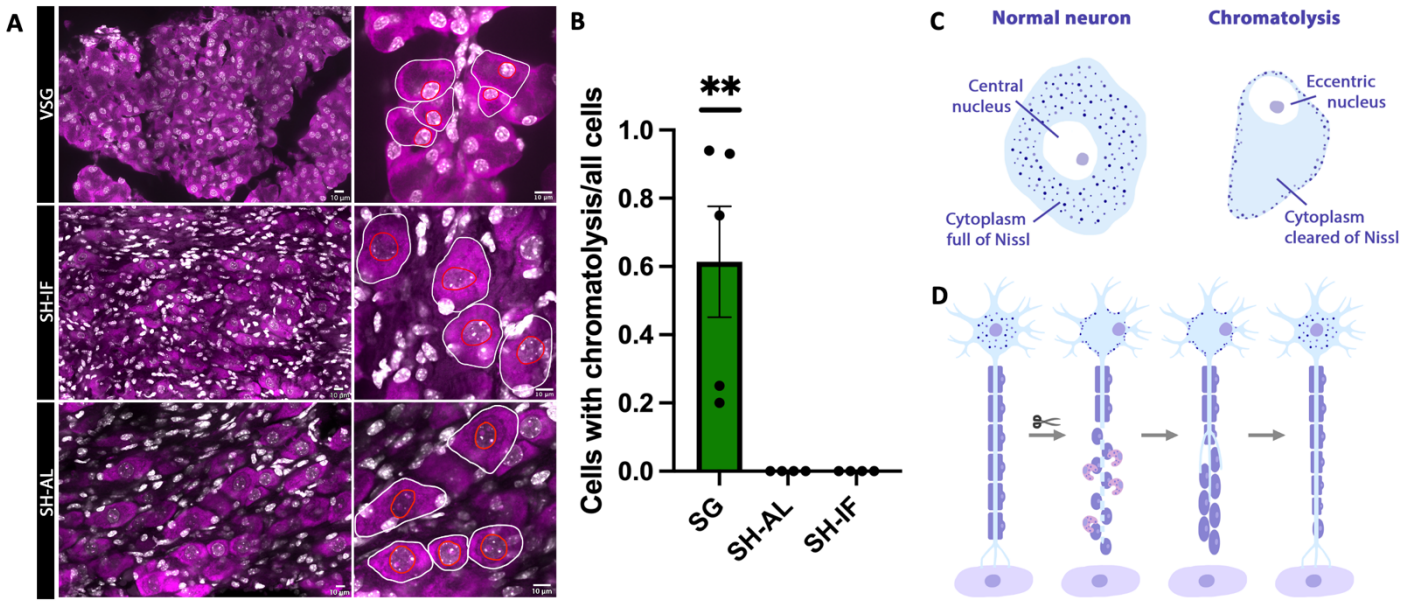
A
VSG
SH-IF
SH-AL
B
**
Cells with chromatolysis/all cells
1.0
0.8
0.6
0.4
0.2
0.0
SG
SH-AL
SH-IF
C
Normal neuron
Chromatolysis
Central nucleus
Cytoplasm full of Nissl
Eccentric nucleus
Cytoplasm cleared of Nissl
D

Figure 2

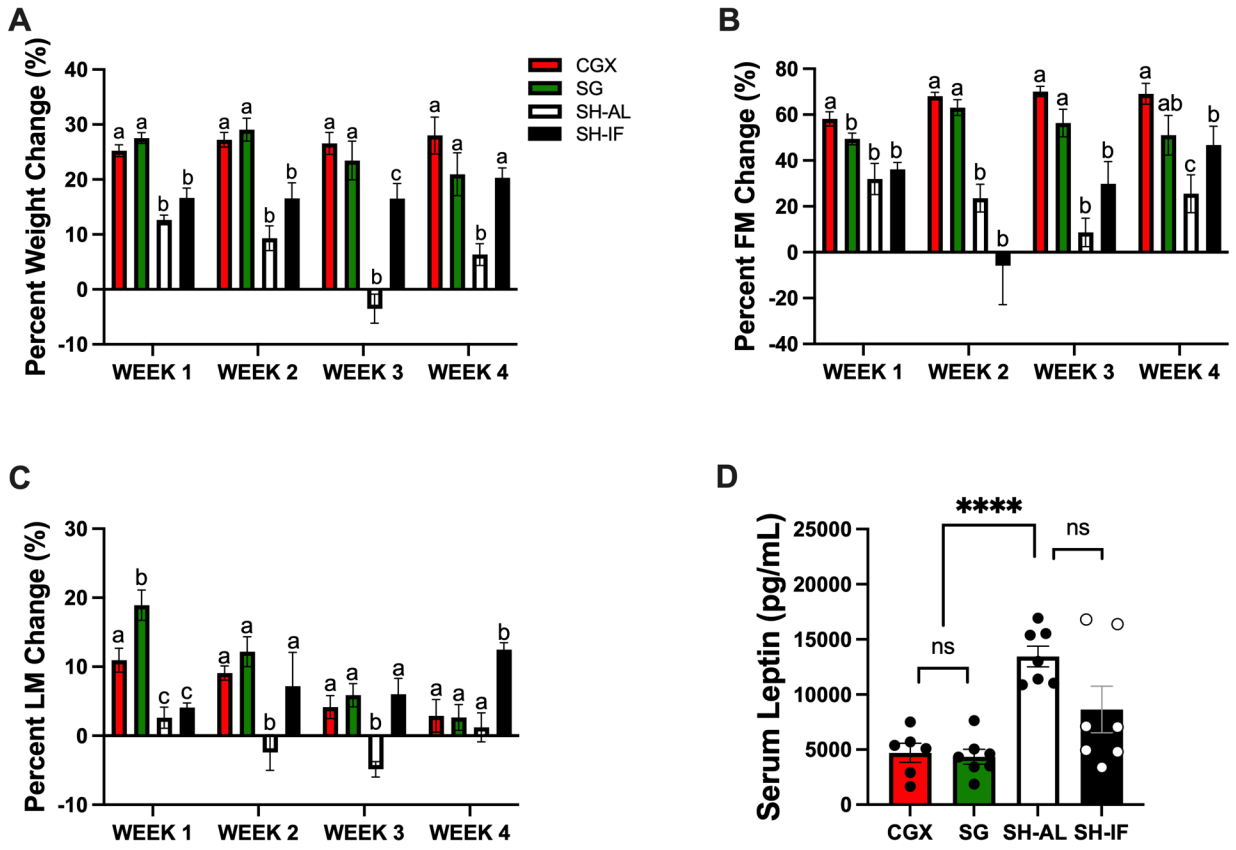
A
Percent Weight Change (%)
CGX
SG
SH-AL
SH-IF
WEEK 1
WEEK 2
WEEK 3
WEEK 4
B
Percent FM Change (%)
C
Percent LM Change (%)
D
Serum Leptin (pg/mL)
****
ns
ns
CGX
SG
SH-AL
SH-IF

Figure 3

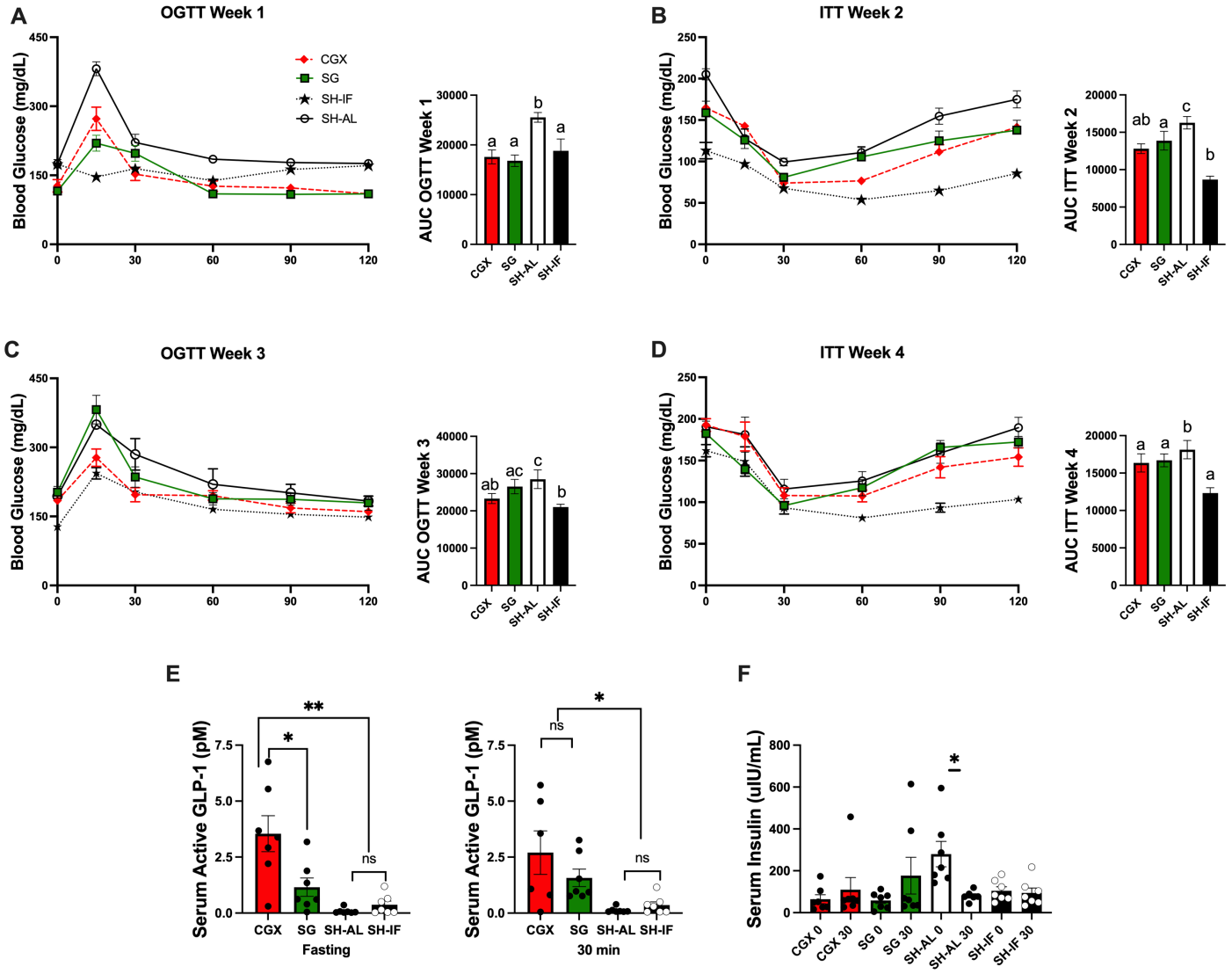
A
OGTT Week 1
Blood Glucose (mg/dL)
CGX
SG
SH-IF
SH-AL
AUC OGTT Week 1
B
ITT Week 2
AUC ITT Week 2
C
OGTT Week 3
AUC OGTT Week 3
D
ITT Week 4
AUC ITT Week 4
E
Serum Active GLP-1 (pM)
Fasting
30 min
ns
F
Serum Insulin (uIU/mL)
CGX 0
CGX 30
SG 0
SG 30
SH-AL 0
SH-AL 30
SH-IF 0
SH-IF 30

Figure 4

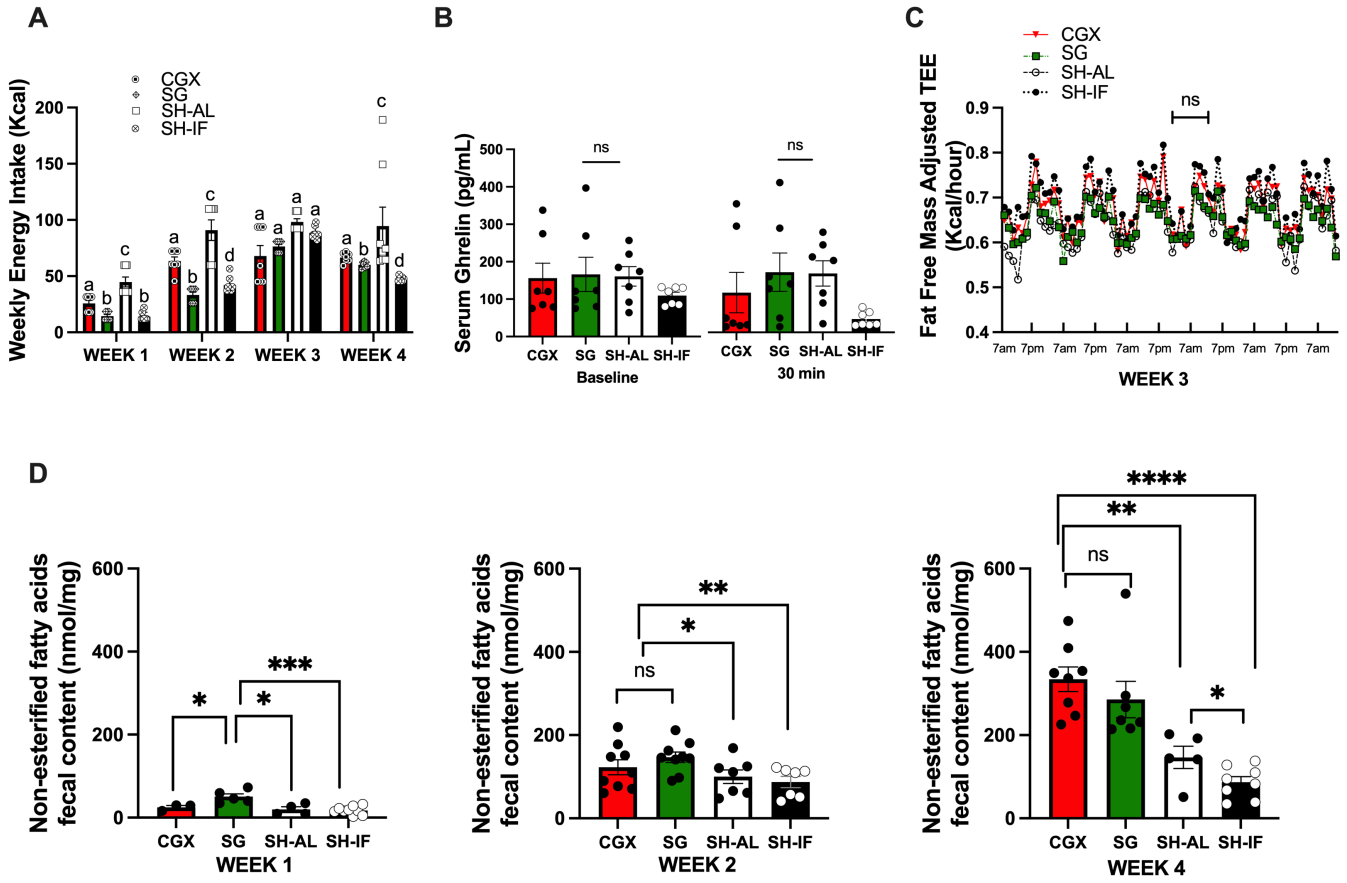
A
Weekly Energy Intake (Kcal)
CGX
SG
SH-AL
SH-IF
WEEK 1
WEEK 2
WEEK 3
WEEK 4
B
Serum Ghrelin (pg/mL)
ns
CGX SG SH-AL SH-IF
Baseline
30 min
C
Fat Free Mass Adjusted TEE (Kcal/hour)
CGX
SG
SH-AL
SH-IF
ns
7am 7pm 7am 7pm 7am 7pm 7am 7pm 7am 7pm 7am
WEEK 3
D
Non-esterified fatty acids fecal content (nmol/mg)
CGX SG SH-AL SH-IF
WEEK 1
WEEK 2
WEEK 4
ns
*
**
***
****

Figure 5

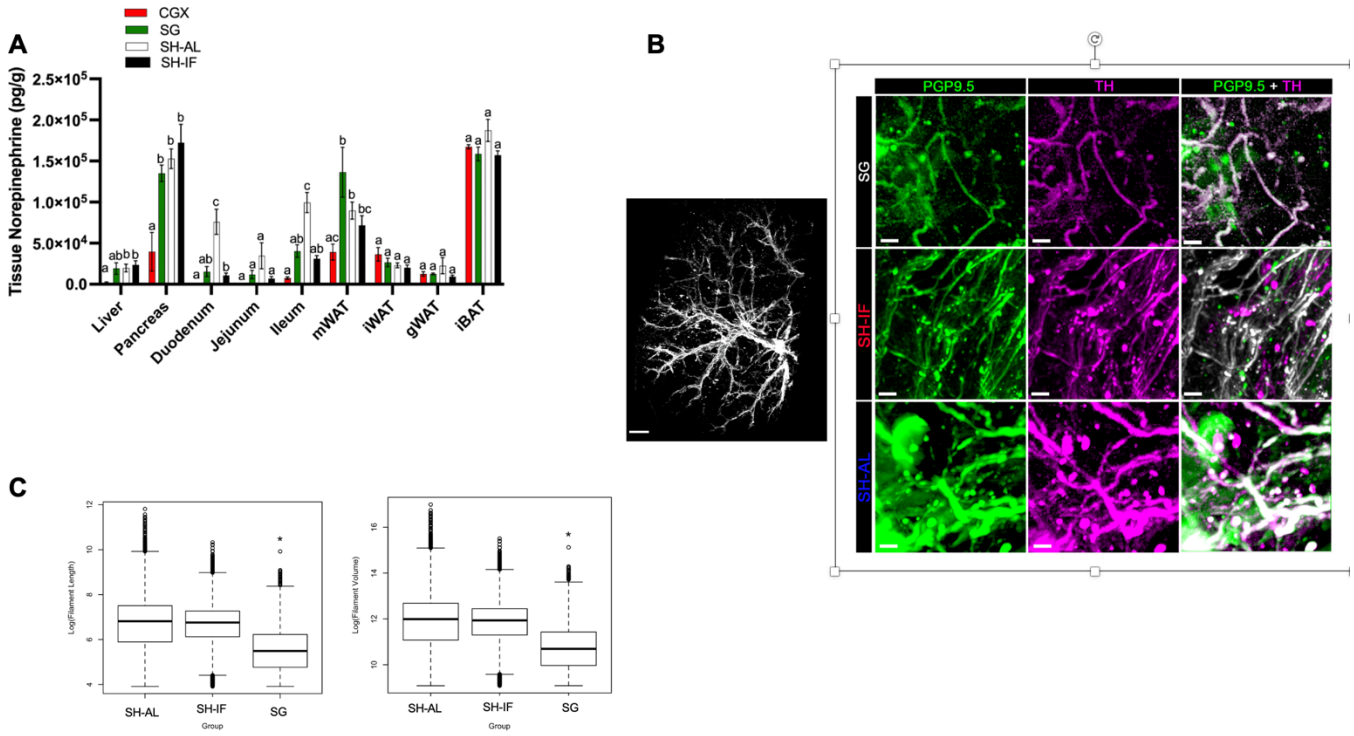
A
CGX
SG
SH-AL
SH-IF
Tissue Norepinephrine (pg/g)
2.5×10^5
2.0×10^5
1.5×10^5
1.0×10^5
5.0×10^4
0.0
Liver
Pancreas
Duodenum
Jejunum
Ileum
mWAT
iWAT
gWAT
iBAT
B
PGP9.5
TH
PGP9.5 + TH
SG
SH-IF
SH-AL
C
Log(Filament Length)
Log(Filament Volume)
SH-AL
SH-IF
SG
Group

Figure 6

Figure Legends

1. **Figure 1.** Schematic representing the celiac-superior mesenteric ganglia and their anatomic boundaries.

2. **Figure 2. Chromatolysis after SG. A.** Confocal images of 20 micrometer-CSMG slices of mice that underwent SG (VSG is interchangeable with SG), sham surgery with caloric restriction with intermittent fasting (SH-IF) and sham surgery ad libitum (SH-AL). Chromatolysis is abundantly present in SG mice, while none is observed in SH-AL and SH-IF mice. Neurons were stained with NeuroTrace 640. Scale bar 10 µm. **B.** Rate of cells with chromatolysis over all cells. One-way ANOVA. N=2-3 mice. **p<0.01. **C.** Schematic depicting chromatolysis. **D.** Schematic showing denervation of specific target organ during chromatolysis, followed by recovery, which is a potential fate for neurons undergoing degenerative changes.

3. **Figure 3. Body weight and body composition changes. A**. Percent Weight change from baseline. For a and b, p<0.0001 on week 1, 2, 3 and 4. For a and c, p<0.05. Two-way ANOVA with multiple comparisons, column factor F (3, 127) = 58.75. **B.** Percent Fat Mass change from baseline. For a and b, p <0.05 for week 1; p<0.001 for week 2; p<0.0001 for week 3, p<0.05 for week 4. For a and c, p<0.001. Two-way ANOVA with multiple comparisons, column factor F (3, 127) = 48.20 **C.** Percent Lean mass change from baseline. For a and b, p<0.05 and a and c, p<0.0001 for week 1. For a and b, p<0.0001 for week 2 and 3; and p<0.001 for week 4. Two-way ANOVA with multiple comparisons, column factor F (3, 127) = 48.20. N=7-14 for each group. **D.** Serum Leptin. One-way ANOVA (p<0.0001 for SH-AL compared to CGX and SG mice).

4. **Figure 4. Glucose homeostasis**. **A and C.** Oral glucose tolerance test on weeks 1 and 3 post-SG, CGX and sham surgery. **B and D.** Insulin tolerance test on weeks 2 and 4. One-way ANOVA was used for analysis of AUC. For A, p<0.001; for B, p<0.0001; for C, p<0.05; for D, p<0.01. N was 8-10 per group, with experiments repeated twice. Serum Active GLP-1 fasting and 30 min after gavage of 200 uL of Ensure. One-way ANOVA. **B.** Serum insulin fasting and 30 min after gavage with Ensure. One-way ANOVA. N=7 mice per group. * for p<0.05; ** for p<0.01.

5. **Figure 5. Food Intake, Total Energy Expenditure and Free Fatty Acid Fecal Content. A.** Weekly energy intake post-surgeries. For a and b, p<0.01 for week 1, p<0.0001 for week 2, and p<0.05 for week 3. For a and c, p<0.01 for week 1, p<0.05 for week 2 and 3. For a and d, p<0.001 for week 2 and p<0.0001 for week 4. Two-way ANOVA with multiple comparisons, column factor F (3, 104) = 31.98. **B.** Serum Ghrelin levels fasting and 30 min after an oral gavage of Ensure. (One-way ANOVA, p>0.05). **C.** Fat Free Mass-Adjusted Total Energy Expenditure, Generalized Linear Model in SPSS. **D.** Non-esterified fatty acid fecal content on weeks 1, 2 and 4. One-way ANOVA. N=7-9; * for p<0.05, ** p<0.01, *** p<0.001 and p<0.0001.

6. **Figure 6. Liver sympathetic innervation. A.** Tissue norepinephrine content by high performance liquid chromatography at 4 weeks post CGX, SG and sham surgery. Two-way ANOVA with multiple comparisons. N=5 per group. For liver, a and b, p<0.05; for pancreas, a and b, p<0.01; for duodenum, a and b, p<0.05, and a and c, p<0.001; for jejunum, p>0.05; for ileum, a and b, p<0.01, and for a and c, p<0.001; for mWAT, a and b, p<0.01, and a and c, p<0.05; for iWAT, gWAT and iBAT, p>0.05. mWAT – mesenteric white adipose tissue; iWAT-inguinal white adipose tissue, gWAT- gonadal white adipose tissue, iBAT- interscapular brown adipose tissue. **B.** Liver iDisco. In black-and-white, whole liver, scale bar 500 µm. Panel shows PGP9.5 (green), TH-labeled neurons (magenta), and the two markers merged (white). Scale bar 10 µm. **C.** Mixed effects model analysis of filament volume and length for sympathetic axons in liver of mice 4 weeks after SG, SH-AL and SH-IF. p<0.05.

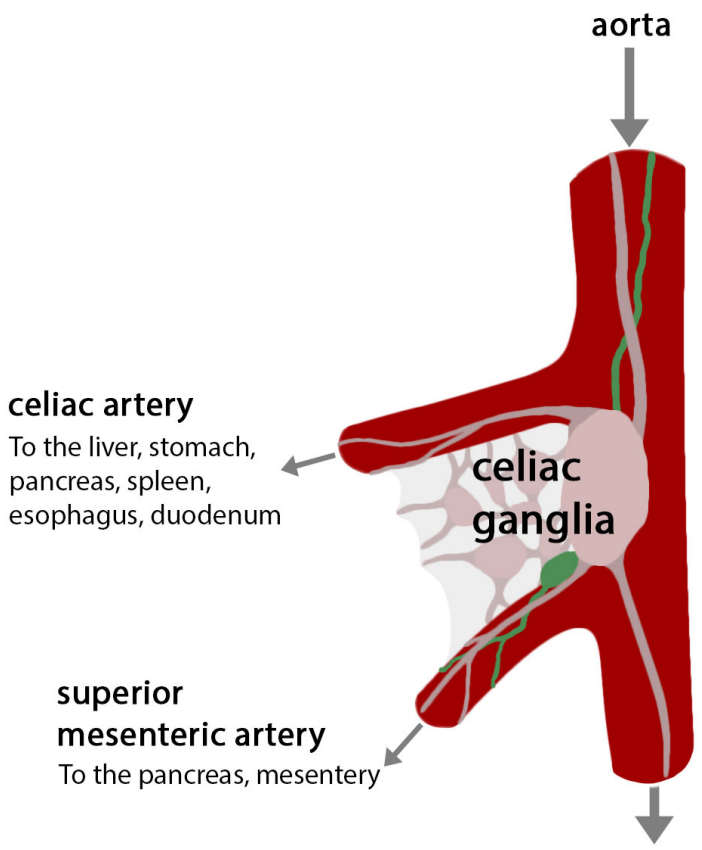
aorta
celiac artery
To the liver, stomach, pancreas, spleen, esophagus, duodenum
celiac ganglia
superior mesenteric artery
To the pancreas, mesentery

Figure 1

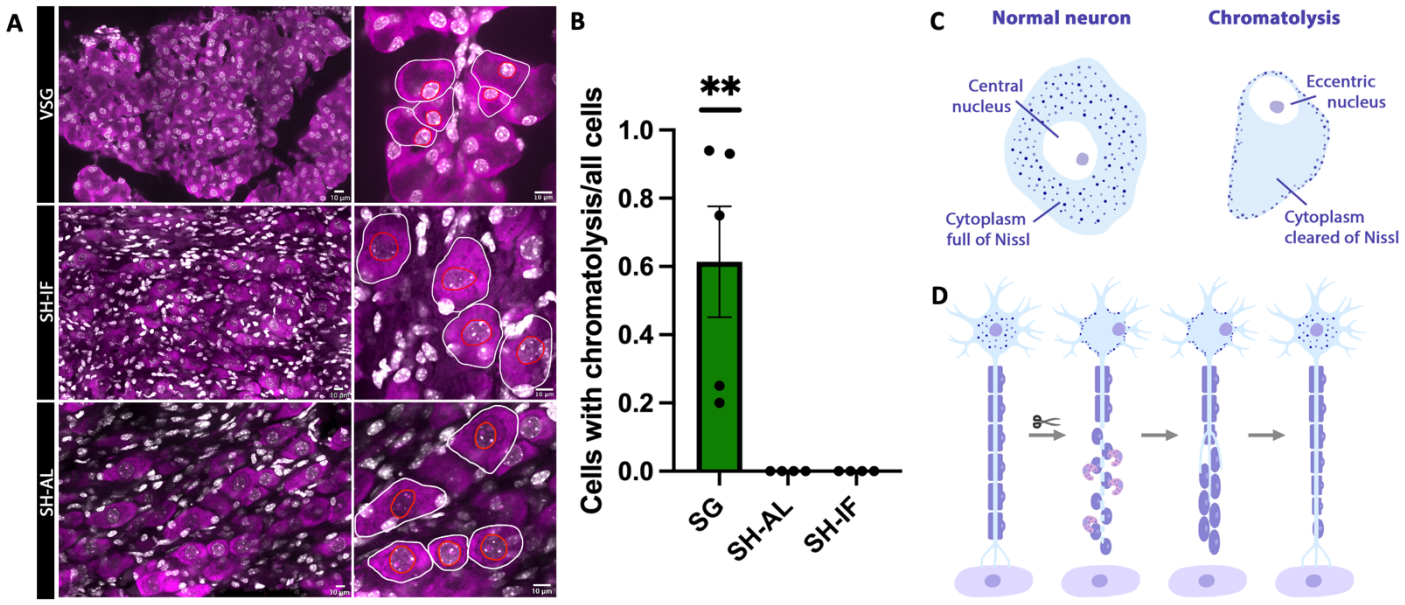
A
VSG
SH-IF
SH-AL
B
**
Cells with chromatolysis/all cells
1.0
0.8
0.6
0.4
0.2
0.0
SG
SH-AL
SH-IF
C
Normal neuron
Chromatolysis
Central nucleus
Cytoplasm full of Nissl
Eccentric nucleus
Cytoplasm cleared of Nissl
D

Figure 2

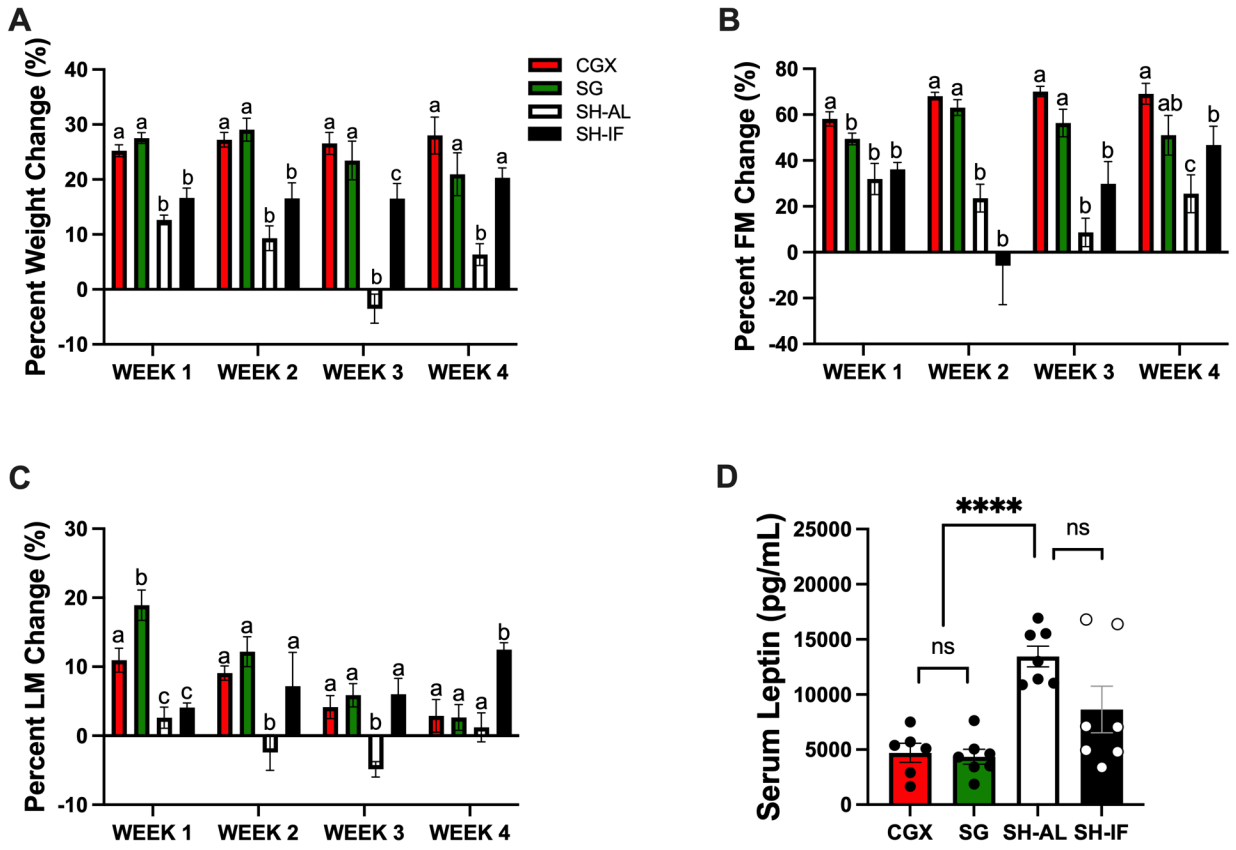
A
Percent Weight Change (%)
CGX
SG
SH-AL
SH-IF
WEEK 1
WEEK 2
WEEK 3
WEEK 4
B
Percent FM Change (%)
C
Percent LM Change (%)
D
Serum Leptin (pg/mL)
****
ns
ns
CGX
SG
SH-AL
SH-IF

Figure 3

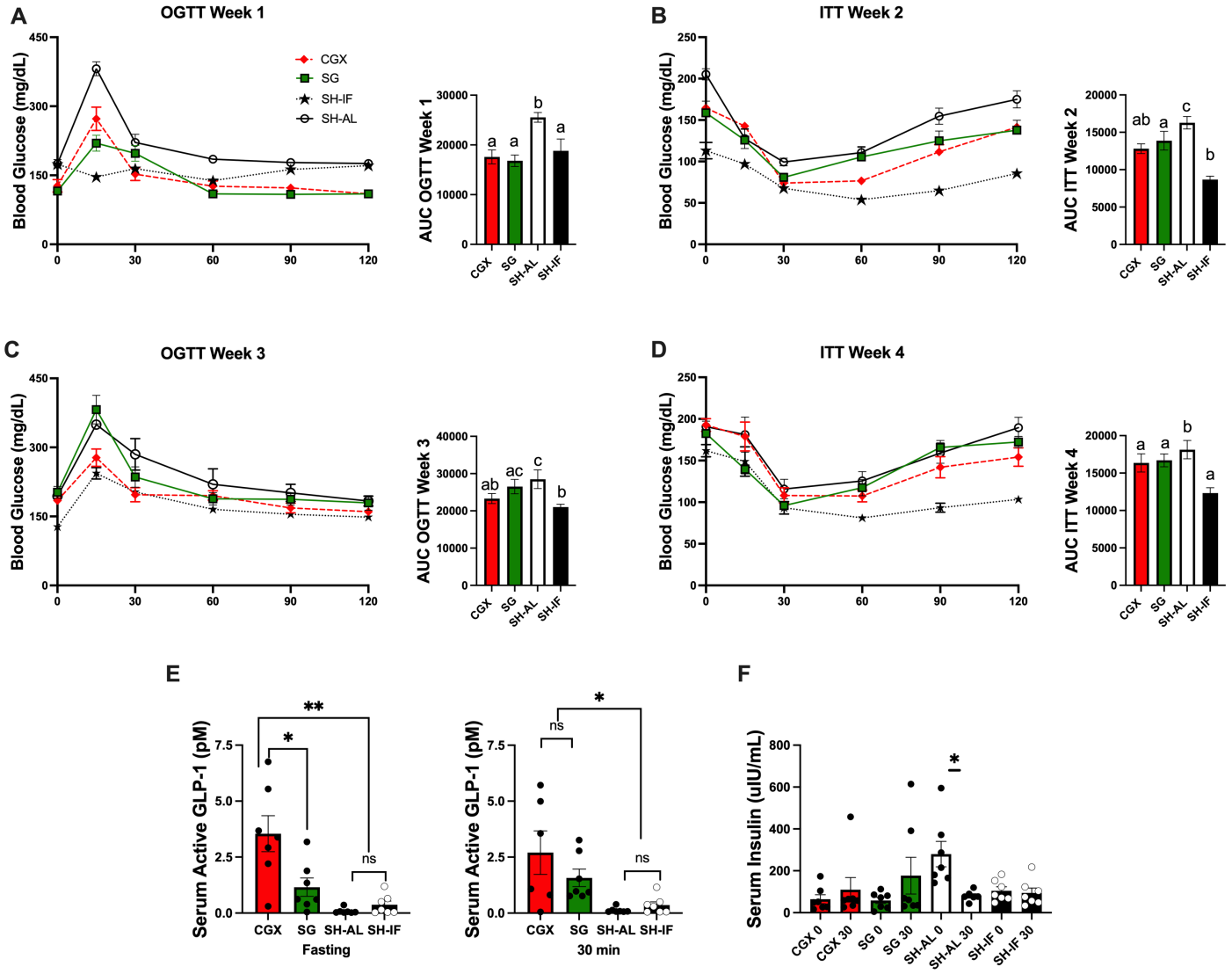
A
OGTT Week 1
Blood Glucose (mg/dL)
CGX
SG
SH-IF
SH-AL
AUC OGTT Week 1
B
ITT Week 2
AUC ITT Week 2
C
OGTT Week 3
AUC OGTT Week 3
D
ITT Week 4
AUC ITT Week 4
E
Serum Active GLP-1 (pM)
Fasting
30 min
ns
F
Serum Insulin (uIU/mL)
CGX 0
CGX 30
SG 0
SG 30
SH-AL 0
SH-AL 30
SH-IF 0
SH-IF 30

Figure 4

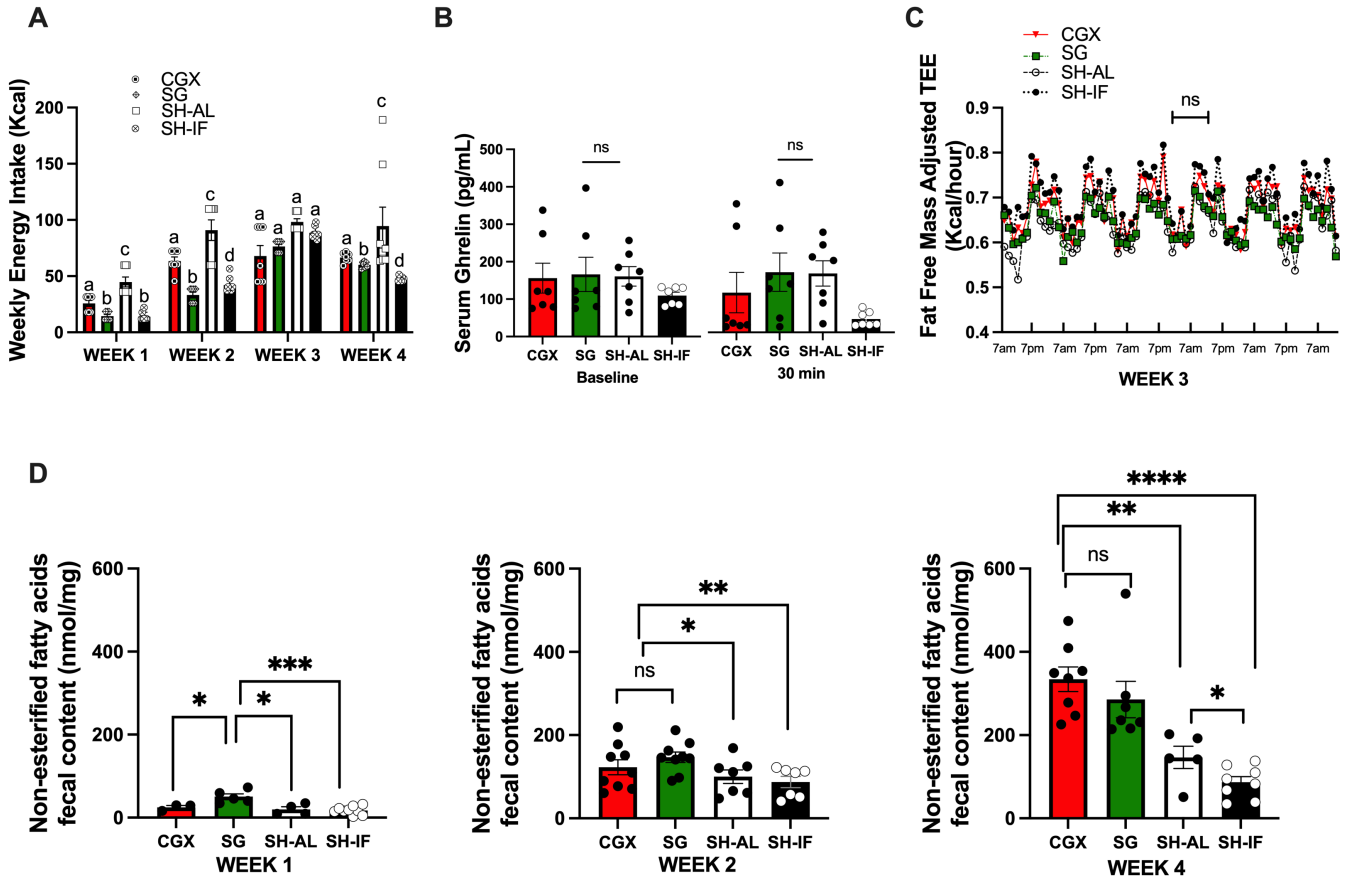
A
Weekly Energy Intake (Kcal)
CGX
SG
SH-AL
SH-IF
WEEK 1
WEEK 2
WEEK 3
WEEK 4
B
Serum Ghrelin (pg/mL)
ns
CGX SG SH-AL SH-IF
Baseline
30 min
C
Fat Free Mass Adjusted TEE (Kcal/hour)
CGX
SG
SH-AL
SH-IF
ns
7am 7pm 7am 7pm 7am 7pm 7am 7pm 7am 7pm 7am
WEEK 3
D
Non-esterified fatty acids fecal content (nmol/mg)
CGX SG SH-AL SH-IF
WEEK 1
WEEK 2
WEEK 4
ns
*
**
***
****

Figure 5

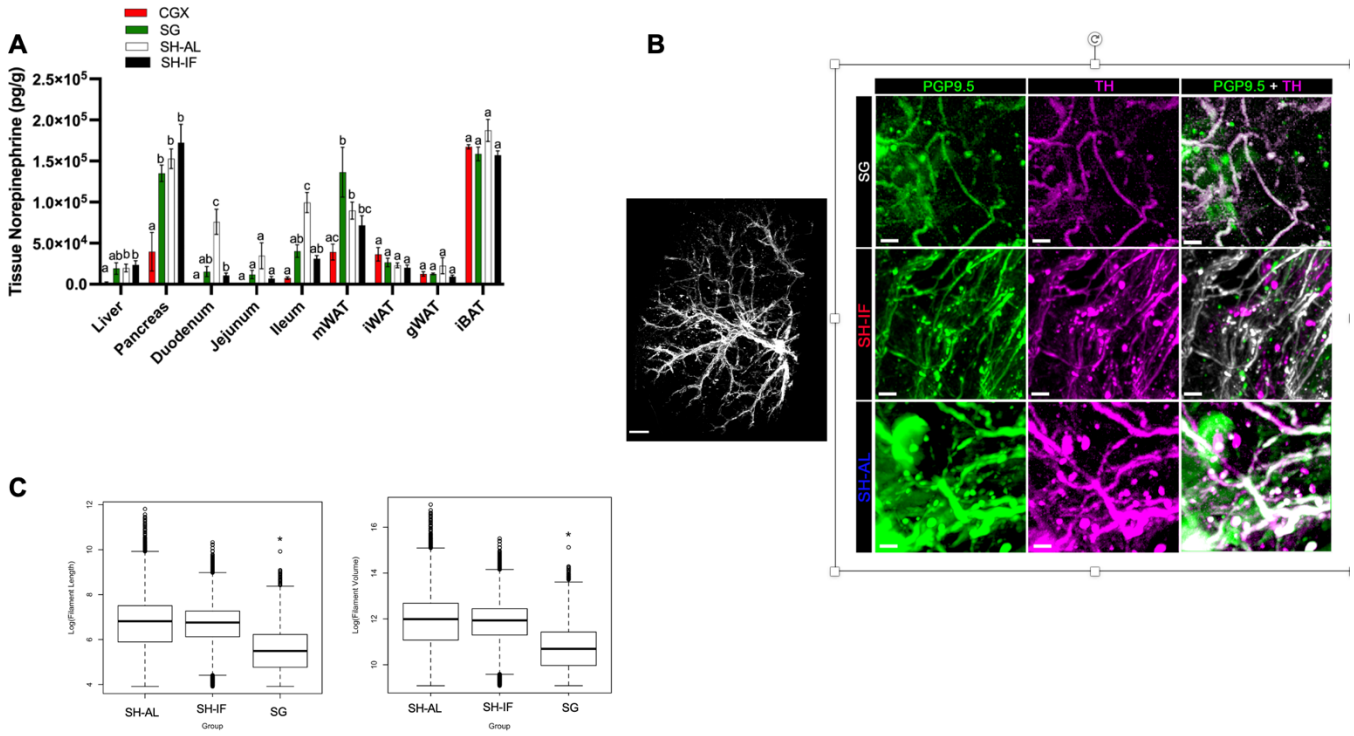
A
CGX
SG
SH-AL
SH-IF
Tissue Norepinephrine (pg/g)
2.5×10^5
2.0×10^5
1.5×10^5
1.0×10^5
5.0×10^4
0.0
Liver
Pancreas
Duodenum
Jejunum
Ileum
mWAT
iWAT
gWAT
iBAT
B
PGP9.5
TH
PGP9.5 + TH
SG
SH-IF
SH-AL
C
Log(Filament Length)
Log(Filament Volume)
SH-AL
SH-IF
SG
Group

Figure 6

Figure Legends

1. **Figure 1.** Schematic representing the celiac-superior mesenteric ganglia and their anatomic boundaries.

2. **Figure 2. Chromatolysis after SG. A.** Confocal images of 20 micrometer-CSMG slices of mice that underwent SG (VSG is interchangeable with SG), sham surgery with caloric restriction with intermittent fasting (SH-IF) and sham surgery ad libitum (SH-AL). Chromatolysis is abundantly present in SG mice, while none is observed in SH-AL and SH-IF mice. Neurons were stained with NeuroTrace 640. Scale bar 10 µm. **B.** Rate of cells with chromatolysis over all cells. One-way ANOVA. N=2-3 mice. **p<0.01. **C.** Schematic depicting chromatolysis. **D.** Schematic showing denervation of specific target organ during chromatolysis, followed by recovery, which is a potential fate for neurons undergoing degenerative changes.

3. **Figure 3. Body weight and body composition changes. A**. Percent Weight change from baseline. For a and b, p<0.0001 on week 1, 2, 3 and 4. For a and c, p<0.05. Two-way ANOVA with multiple comparisons, column factor F (3, 127) = 58.75. **B.** Percent Fat Mass change from baseline. For a and b, p <0.05 for week 1; p<0.001 for week 2; p<0.0001 for week 3, p<0.05 for week 4. For a and c, p<0.001. Two-way ANOVA with multiple comparisons, column factor F (3, 127) = 48.20 **C.** Percent Lean mass change from baseline. For a and b, p<0.05 and a and c, p<0.0001 for week 1. For a and b, p<0.0001 for week 2 and 3; and p<0.001 for week 4. Two-way ANOVA with multiple comparisons, column factor F (3, 127) = 48.20. N=7-14 for each group. **D.** Serum Leptin. One-way ANOVA (p<0.0001 for SH-AL compared to CGX and SG mice).

4. **Figure 4. Glucose homeostasis**. **A and C.** Oral glucose tolerance test on weeks 1 and 3 post-SG, CGX and sham surgery. **B and D.** Insulin tolerance test on weeks 2 and 4. One-way ANOVA was used for analysis of AUC. For A, p<0.001; for B, p<0.0001; for C, p<0.05; for D, p<0.01. N was 8-10 per group, with experiments repeated twice. Serum Active GLP-1 fasting and 30 min after gavage of 200 uL of Ensure. One-way ANOVA. **B.** Serum insulin fasting and 30 min after gavage with Ensure. One-way ANOVA. N=7 mice per group. * for p<0.05; ** for p<0.01.

5. **Figure 5. Food Intake, Total Energy Expenditure and Free Fatty Acid Fecal Content. A.** Weekly energy intake post-surgeries. For a and b, p<0.01 for week 1, p<0.0001 for week 2, and p<0.05 for week 3. For a and c, p<0.01 for week 1, p<0.05 for week 2 and 3. For a and d, p<0.001 for week 2 and p<0.0001 for week 4. Two-way ANOVA with multiple comparisons, column factor F (3, 104) = 31.98. **B.** Serum Ghrelin levels fasting and 30 min after an oral gavage of Ensure. (One-way ANOVA, p>0.05). **C.** Fat Free Mass-Adjusted Total Energy Expenditure, Generalized Linear Model in SPSS. **D.** Non-esterified fatty acid fecal content on weeks 1, 2 and 4. One-way ANOVA. N=7-9; * for p<0.05, ** p<0.01, *** p<0.001 and p<0.0001.

6. **Figure 6. Liver sympathetic innervation. A.** Tissue norepinephrine content by high performance liquid chromatography at 4 weeks post CGX, SG and sham surgery. Two-way ANOVA with multiple comparisons. N=5 per group. For liver, a and b, p<0.05; for pancreas, a and b, p<0.01; for duodenum, a and b, p<0.05, and a and c, p<0.001; for jejunum, p>0.05; for ileum, a and b, p<0.01, and for a and c, p<0.001; for mWAT, a and b, p<0.01, and a and c, p<0.05; for iWAT, gWAT and iBAT, p>0.05. mWAT – mesenteric white adipose tissue; iWAT-inguinal white adipose tissue, gWAT- gonadal white adipose tissue, iBAT- interscapular brown adipose tissue. **B.** Liver iDisco. In black-and-white, whole liver, scale bar 500 µm. Panel shows PGP9.5 (green), TH-labeled neurons (magenta), and the two markers merged (white). Scale bar 10 µm. **C.** Mixed effects model analysis of filament volume and length for sympathetic axons in liver of mice 4 weeks after SG, SH-AL and SH-IF. p<0.05.